Apical Sterol-rich Membranes Are Essential for Localizing Cell End Markers That Determine Growth Directionality in the Filamentous Fungus *Aspergillus nidulans*

Norio Takeshita, Yuhei Higashitsuji, Sven Konzack, and Reinhard Fischer

Applied Microbiology, University of Karlsruhe, D-76187 Karlsruhe, Germany

In filamentous fungi, hyphal extension depends on the continuous delivery of vesicles to the growing tip. Here, we describe the identification of two cell end marker proteins, TeaA and TeaR, in *Aspergillus nidulans*, corresponding to Tea1 and Mod5 in *Schizosaccharomyces pombe*. Deletion of *teaA* or *teaR* caused zig-zag-growing and meandering hyphae, respectively. The Kelch-repeat protein TeaA, the putatively prenylated TeaR protein, and the formin SepA were highly concentrated in the Spitzenkörper, a vesicle transit station at the tip, and localized along the tip membrane. TeaA localization at tips depended on microtubules, and TeaA was required for microtuble convergence in the hyphal apex. The CENP-E family kinesin KipA was necessary for proper localization of TeaA and TeaR, but not for their transportation. TeaA and TeaR localization were interdependent. TeaA interacted in vivo with TeaR, and TeaA colocalized with SepA. Sterol-rich membrane domains localized at the tip in *teaA* and *teaR* mutants like in wild type, and filipin treatment caused mislocalization of both proteins. This suggests that sterol-rich membrane domains determine cell end factor destinations and thereby polarized growth.

INTRODUCTION

The generation of asymmetry and polarization of cells is important in all kingdoms, and their molecular mechanisms are studied in different organisms. The diversity of cell shapes and functions suggests the development of different ways to generate and maintain polarity. However, it turns out that core mechanisms are conserved and that they may include the localized assembly of signaling complexes, the rearrangement of the cytoskeleton, the mobilization of proteins from intracellular pools, and the targeted vesicle delivery to sites of membrane growth (Nelson, 2003). One important early step for the generation of asymmetry is the local deposition of so-called landmark proteins at the surface of a cell, which serve as initiation sites for the localized assembly of additional proteins and thereby as a key for the reorientation of the cytoskeleton. In eukaryotes, polarity establishment is well studied at the molecular level in *Saccharomyces cerevisiae* and *Schizosaccharomyces pombe* (Chang and Peter, 2003).

In *S. pombe*, a visual mutant screening for strains with bent and T-shaped cells instead of cigar-like, straight cells led to the identification of one crucial component, the Kelch-repeat protein Tea1 (Snell and Nurse, 1994; Mata and Nurse, 1997). This protein is transported along microtubules (MTs) to their plus ends by the CENP-E family kinesin Tea2, and it is delivered to the cell ends by the growing MTs (Browning *et al.*, 2000, 2003). At the pole, Tea1 is anchored at the membrane by a second landmark protein, Mod5, which itself is

prenylated, and through this lipid moiety it is attached to the membrane (Snaith and Sawin, 2003). Because Tea1 and Mod5 accumulate at the growing cell end, they were named cell end markers. Along with a number of additional components, a large protein complex is formed, which recruits the formin For3 (Martin and Chang, 2003). For3 is required for actin cable formation; thus, it is crucial for the orientation of the actin cytoskeleton toward the growing cell end (Martin and Chang, 2006). Actin cables are required for polarized secretion of vesicles and hence membrane enlargement and secretion of cell wall-synthesizing enzymes (Montegi *et al.*, 2001).

In *S. cerevisiae*, several membrane-associated landmark proteins, such as Bud8 or Bud9, were described, which are absent from the *S. pombe* proteome (Pringle *et al.*, 1995; Zahner *et al.*, 1996; Kang *et al.*, 2001). Associated to the landmark proteins in *S. cerevisiae*, and localized at the emerging bud, is a large protein complex named polarisome that consists of a scaffold protein, Spa2; several other proteins; and characteristically the formin Bni1 (Sheu *et al.*, 1998). The kelch-domain protein Tea1 is conserved in *S. cerevisiae* (Kel1), where it is involved in mating projection formation (Philips and Herskowitz, 1998). In contrast, Mod5 is absent from the budding yeast proteome (Philips and Herskowitz, 1998; Snaith and Sawin, 2003).

If the polarized deposition of landmark proteins represents the crucial step in marking the zone of growth, the question arises which molecules or factors guide the proteins to their destination. There is increasing evidence that different membrane compositions or organizations may be important marks for the polarization of cells. It is known that eukaryotic membranes are differentiated into different functional areas, named lipid rafts (Rothberg *et al.*, 1990; Rajendra and Simons, 2005). They can vary in their lipid composition, and one type is characterized by a high content of sterols and is also found in fungi (Alvarez *et al.*, 2007). It

has been shown recently that the polarization of the membrane contributes to polar growth in *Candida albicans* (Martin and Konopka, 2004), but a link between the protein complexes described above and such membrane microdomains is missing.

Polarized growth is the dominant growth form of filamentous fungi. In these organisms, a structure localized in the apical dome of the hyphae and involved in polarized growth has been known for a long time, and it is named the Spitzenkörper (Girbardt, 1957). It represents an accumulation of vesicles and it determines growth direction of fungal hyphae (Grove and Bracker, 1970; Riquelme *et al.*, 1998). The exact structure and organization are still not completely understood. However, it could be an organelle-like structure rather than only an accumulation of vesicles (Wright *et al.*, 2007). Indeed, actin filaments have been observed in freeze-substituted samples (Howard, 1981). Molecular analyses in *Ashbya gossypii* and *Aspergillus nidulans* revealed that polarisome components may be components of the Spitzenkörper (Sharpless and Harris, 2002; Knechtle *et al.*, 2003; Harris *et al.*, 2005). Conversely, Crampin *et al.* (2005) described the Spitzenkörper as a structure distinct from the polarisome in *C. albicans*. They describe several components typical for the *S. cerevisiae* polarisome, such as Spa2 and Bud6, localized to a cap-like structure close to the cytoplasmic membrane, whereas the formin Bni1 was localized to the Spitzenkörper. Spa2 and Bud6 orthologues, SpaA and BudA, respectively, were also studied in *A. nidulans* (Virag and Harris, 2006). Deletion of either had an effect on polarized growth, but whereas SpaA could be localized at the tip, overlapping with the Spitzenkörper, BudA was only detectable at septa, indicating a role during cytokinesis. Several other *S. cerevisiae* landmark proteins are missing in filamentous fungal proteomes (Harris and Momany, 2004). Orthologues of the *S. pombe* cell end markers and the associated machinery have not yet been studied in filamentous fungi, but genome analyses revealed that one crucial component, the prenylated Mod5 protein, was not conserved in any filamentous fungus (Snaith and Sawin, 2003).

Previously, we showed that the deletion of the CENP-E family kinesin KipA, corresponding to Tea2 in *S. pombe* caused meandering hyphae (Konzack *et al.*, 2005). Here, we show that a protein with a similar function as Mod5, named TeaR, does exist in *A. nidulans*, and we show that TeaR together with a Tea1 orthologue, TeaA is involved in the initiation of polarized growth and the maintenance of straight-growing hyphae. We studied the relationship between KipA, the two cell end markers, and the formin SepA. Interestingly, the polarized localization of TeaA and TeaR depends on sterol-rich membrane domains.

MATERIALS AND METHODS

Strains, Plasmids and Culture Conditions

Supplemented minimal (MM) and complete media (CM) for *A. nidulans* were prepared as described, and standard strain construction procedures are described by Hill and Käfer (2001). A list of *A. nidulans* strains used in this study is given in Table 1. Standard laboratory *Escherichia coli* strains (XL-1 blue, Top 10 F') were used. Plasmids are listed in Table 2.

Molecular Techniques

Standard DNA transformation procedures were used for *A. nidulans* (Yelton *et al.*, 1984) and *Escherichia coli* (Sambrook and Russel, 1999). For polymerase chain reaction (PCR) experiments, standard protocols were applied using a capillary Rapid Cycler (Idaho Technology, Idaho Falls, ID) for the reaction cycles. DNA sequencing was done commercially (MWG Biotech, Ebersberg, Germany). Genomic DNA was extracted from *A. nidulans* with the DNeasy Plant Mini kit (QIAGEN, Hilden, Germany). DNA analyses (Southern hybridizations) were performed as described by Sambrook and Russel (1999).

Deletion of teaA and teaR

teaA flanking regions were amplified by PCR using genomic DNA and the primers teaA1-linke-Fla-for (5'-GAGAAACGTCCATACTTCTG-3') and teaA2-linke-Fla-rev-SfiI1 (5'-TGGTGGCCATCTAGGCCCCAGGAAACATTG-CTTTC-3') for the upstream region of *teaA* and teaA3-rechte-Fla-for-SfiI2 (5'-AATAGGCCTGAGTGGCCAACAGTGCAGTGTCAC-3') and teaA4-rechte-Fla-rev (5'-CCATCTCTGGTTCGGCTTAC-3') for the downstream region, and they were cloned into pCR2.1-TOPO to generate pSK74 and pSK75, respectively. The SfiI restriction sites are underlined. In a three-fragment-ligation, the *argB*-gene from plasmid pSK70 was ligated between the two *teaA*-flanking regions, resulting in vector pSK76. The deletion cassette was amplified with the primers teaA-for-n (5'-GAAGAACCAGCAGACTTCTG-3') and teaA-rev-n (5'-CTGGTCTGCTGCTGAAATG-3'), and the resulting PCR product was transformed into the arginin-auxotrophic *A. nidulans* strain SRF200.

teaR flanking regions were amplified by PCR using genomic DNA and the primers teaR1-KpnI (5'-GGTACCAGATGGCTGTTGAAGTTGTC-3') and teaR2-BamHI (5'-GGATCCAGCGTCCAACAGAAGAATGT-3') for the upstream region of *teaR* and teaR3-NotI (5'-GCGGCCGCTACCTCTGCTATTG-CAAGTAT-3') and teaR4-XbaI (5'-TCTAGATCTTGCTGGCCTTGCAGTA-3') for the downstream region and cloned into pCR2.1-TOPO, to generate pNT12 and pNT13, respectively. The restriction sites are underlined. The two *teaR*-flanking regions were ligated in upstream and downstream of the *pyr4* marker in pNRSTE1, generating pNT14. This plasmid was cut with KpnI and XbaI, generating a fragment containing *pyr4* flanked by *teaR* sequences. This fragment was transformed into the uracil-auxotrophic SRF200.

Transformants were screened by PCR for the homologous integration event. Single integration of the construct was confirmed by Southern blotting (data not shown). One *teaA*- and one *teaR*-deletion strain were selected from the transformants and named SSK91 and SNT33, respectively. The coupling of the observed phenotypes with the gene-deletion events was confirmed by crosses, recomplementation with *tea*- or *teaR*-derived clones, and by down-regulation of the genes through the inducible *alcA* promoter (see below).

Tagging of Proteins with Green Fluorescent Protein (GFP) and Monomeric Red Fluorescent Protein (mRFP) 1

To create an N-terminal GFP fusion construct of TeaA, a 0.7-kb N-terminal fragment of *teaA* (starting from ATG) was amplified from genomic DNA, with the primers tea_Efi_for (5'-GGGGCGCGCCCATGGCGTTCCTCTTTAAAT-CAAAG-3') and tea_Efi_rev (5'-GGTTAATTAATTGGTATCACCGCCAAA-GACGA-3') and cloned into pCR2.1-TOPO, yielding pNT1. The restriction sites are underlined. The AscI–PacI fragment from pNT1 was subcloned into the corresponding sites of pCMB17apx, yielding pNT5. To create an N-terminal mRFP1 fusion construct of TeaA, the AscI-PacI fragment from pNT1 was subcloned into the corresponding sites of pDM8, yielding pNT6. To produce TeaA N-terminally tagged with mRFP1 under the native promoter, a 1.5-kb fragment of the *teaA* promoter was amplified from genomic DNA with the primers teaA-proEcoRI (5'-GGGAATTCACAAAGGCCAACAGGTGA-TC-3') and teaA-proKpnI (5'-GGGTACCCGTGAAATCTTATATCGTATAC-3'), digested with EcoRI and KpnI, and ligated with EcoRI-KpnI–digested pNT6, yielding pNT28 (*alcA* promoter replaced with the *teaA* promoter in pNT6). Using the same approach as for TeaA, N-terminal GFP fusion constructs of TeaR and SepA were created. The primer set used for TeaR was tear_Efi_for (5'-GGGGCGCGCCCATGGCGGGTACAGCTAC-3') and tear_Efi_rev (5'-GGTTA-ATTAAATACTTGATGTACTAGAACC-3'). The PCR fragment was cloned into pCR2.1-TOPO and subsequently into pCMB17apx, yielding plasmid pNT7. A 1.5-kb fragment of the *teaR* promoter was amplified with the primers teaR-proEcoRI (5'-GAATTCGGCTTGGCTATATGGTCTGG-3') and teaR-proKpnI (5'-GGTACCCAGCGTCCAACAGAAGAATG-3') and ligated into EcoRI-KpnI–digested pNT7, yielding pNT30 (*alcA* promoter replaced with the *teaR* promoter in pNT7). The primer set used for SepA was sepA_Efi_for (5'-GGGGCGCGCCCATGCCGACATCCGATAAAT-3') and sepA_Efi_rev (5'-GGTTAATTAACTATCCATGCGTCTCTCGA-3'). The PCR fragment was cloned into pCR2.1-TOPO and subsequently into pCMB17apx, yielding pNT9. All plasmids were transformed into the uracil-auxotrophic TN02A3 (Δ*nkuA*). The integration events were confirmed by PCR and Southern blotting (data not shown).

To introduce a point mutation in the TeaR CAAX motif, the *teaR*-open reading frame (ORF) was amplified with primers, tear_Efi_for (5'-GGGGCGCGCCCATGGCGGGTACAGCTAC-3') and teaR-full-c-mut (5'-TTAATTAATCACATCACGATGCCGCATC-3'). The point mutation site is underlined and in bold. The PCR fragment was cloned into pCR2.1-TOPO and subsequently into pCMB17apx, yielding pNT32 (cysteine in the CAAX motif was replaced by glycine). As a control, the *teaR*-ORF was amplified with primers teaR_Efi_for (5'-GGGGCGCGCCCATGGCGGGTACAGCTAC-3') and teaR-full-c (5'-TTAATTAATCACATCACGATGCAGCATC-3'), and cloned into pCR2.1-TOPO and subsequently into pCMB17apx, yielding pNT31. To create TeaR tagged with GFP at the C terminus, the *teaR*-ORF was amplified with primers TeaR-pENTR-for (5'-CACCATGGCGGGTACAGC-TACG-3') and TeaR-pENTR-rev (5'-CATCACGATGCAGCATCC-3'), and cloned into the pENTR/TOPO vector (Invitrogen, NV Leek, The Nether-

Table 1. *A. nidulans* strains used in this study

Strain	Genotype	Source
SRF200	*pyrG89; ΔargB::trpCΔB; pyroA4; veA1*	Karos and Fischer (1999)
TN02A3	*pyrG89; argB2, nkuA::argB; pyroA4*	Nayak *et al.* (2005)
GR5	*pyrG89; wA3; pyroA4; veA1*	Waring *et al.* (1989)
RMS011	*pabaA1, yA2; ΔargB::trpCΔB; veA1*	Stringer *et al.* (1991)
SRL1	*ΔkipA::pyr4; pyrG89; pyroA4; veA1 (ΔkipA)*	Konzack *et al.* (2005)
SSK13	*pabaA1; wa3; ΔkipA::pyr4; veA1 (ΔkipA)*	Konzack *et al.* (2005)
SSK44	*wa3; ΔargB::trpCΔB; ΔkipA::pyr4; veA1 (ΔkipA)*	Konzack *et al.* (2005)
SJW02	*wA3; pyroA4; ΔargB::trpCΔB; alcA(p)::GFP::tubA; veA1 (GFP-MTs)*	J. Warmbold (Marburg, Germany)
SSK91	SRF200 transformed with pSK76, *ΔteaA::argB; pyrG89; ΔargB::trpCΔB; pyroA4; veA1 (ΔteaA)*	Konzack *et al.* (2005)
SSK92	*pyrG89; wA3; pyroA4;; alcA(p)::GFP::kipA; veA1 (GFP-KipA)*	(Konzack *et al.* (2005)
SSK114	*pyrG89; wA3; pyroA4;; alcA(p)::GFP::kipA-rigor; veA1 (GFP-KipA-rigor)*	Konzack *et al.* (2005)
SNR1	*ΔkinA::pyr4; pyrG89, yA2; ΔargB::trpCΔB; pyroA4; (ΔkinA)*	Requena *et al.* (2001)
SNT30	SSK91 transformed with pI4 (ΔteaA)	This study
SNT33	SRF200 transformed with pNT14, *ΔteaA::argB; pyrG89; ΔargB::trpCΔB; pyroA4; veA1 (ΔteaR)*	This study
SNT34	SNT33 transformed with pI4 (ΔteaR)	This study
SNT35	SNT33 transformed with pDC1 (ΔteaR)	This study
SNT14	SSK44 crossed to SSK91 (ΔkipA, ΔteaA)	This study
SNT40	SRL1 crossed to SNT34 (ΔkipA, ΔteaR)	This study
SNT39	SNT30 crossed to SNT33 (ΔteaA, ΔteaR)	This study
SNT4	TN02A3 transformed with pNT5, (GFP-TeaA)	This study
SNT13	SNT4 crossed to RSM011, (GFP-TeaA)	This study
SNT5	TN02A3 transformed with pNT6, (mRFP1-TeaA)	This study
SNT15	SNT5 crossed to RSM011, (mRFP1-TeaA)	This study
SNT49	TN02A3 transformed with pNT28, (teaA(p)-mRFP1-TeaA)	This study
SNT52	SNT49 crossed to RSM011, (teaA(p)-mRFP1-TeaA)	This study
SNT26	TN02A3 transformed with pNT7, (GFP-TeaR)	This study
SNT55	TN02A3 transformed with pNT30, (teaR(p)-GFP-TeaR)	This study
SNT61	SNT33 transformed with pNT32 and pDC1, (ΔteaR, GFP-TeaR-CAAX-mutant)	This study
SNT60	SNT33 transformed with pNT31 and pDC1, (ΔteaR, GFP-TeaR)	This study
SNT46	SNT33 transformed with pNT21 (ΔteaR, TeaR-GFP)	This study
SNT21	SJW02 transformed with pDC1, (GFP-MTs)	This study
SNT22	SNT21 crossed to SNT15, (GFP-MTs, mRFP1-TeaA)	This study
SNT31	SNT30 crossed to SJW02, (GFP-MTs, ΔteaA)	This study
SNT23	SSK92 crossed to SNT15, (GFP-KipA, mRFP1-TeaA)	This study
SNT41	SRL1 crossed to SNT15, (ΔkipA, mRFP1-TeaA)	This study
SNT50	SSK44 crossed to SNT49, (ΔkipA, teaA(p)-mRFP1-TeaA)	This study
SNT17	SSK114 transformed with pI4, (GFP-KipA-rigor)	This study
SNT51	SNT17 crossed to SNT49, (GFP-KipA-rigor, teaA(p)-mRFP1-TeaA)	This study
SNT28	TN02A3 transformed with pNT9, (GFP-SepA)	This study
SNT57	SNT28 crossed to SNT52, (GFP-SepA, teaA(p)-mRFP1-TeaA)	This study
SNT56	SNT26 crossed to SNT52, (GFP-TeaR, teaA(p)-mRFP1-TeaA)	This study
SNT27	SNT15 crossed to SNT26, (GFP-TeaR, mRFP1-TeaA)	This study
SNT58	TN02A3 transformed with pNT29 and pYH03, (YFP^N-SepA and teaA(p)-YFP^C-TeaA)	This study
SNT59	TN02A3 transformed with pNT29 and pYH04, (YFP^N-TeaR and teaA(p)-YFP^C-TeaA)	This study
SYH05	TN02A3 transformed with pYH01 and pYH05, (YFP^N-TeaA and YFP^C-KipA)	This study
SYH06	TN02A3 transformed with pYH03 and pYH05, (YFP^N-SepA and YFP^C-KipA)	This study
SYH07	TN02A3 transformed with pYH04 and pYH05, (YFP^N-TeaR and YFP^C-KipA)	This study
SYH08	TN02A3 transformed with pYH04 and pYH14, (YFP^N-TeaR and YFP^C-SepA)	This study
SNT43	SNT26 crossed to SSK13, (GFP-TeaR, ΔkipA)	This study
SNT42	SNT13 crossed to SNT35, (GFP-TeaA, ΔteaR)	This study
SNT53	SNT49 crossed to SNT34, (teaA(p)-mRFP1-TeaA, ΔteaR)	This study
SNT32	SNT30 crossed to SNT26, (GFP-TeaR, ΔteaA)	This study
SNT62	SNR3 crossed to SNT52, (ΔkinA, teaA(p)-mRFP1-TeaA)	This study

lands), yielding pNT16. The fusion of TeaR with GFP at the C terminus was done with the GATEway cloning system and vector pMT-sGFP (Toews *et al.*, 2004), yielding pNT21.

For bimolecular fluorescence complementation (BiFC) analyses, the N-terminal half of yellow fluorescent protein (YFP^N) or the C-terminal half of YFP (YFP^C) was fused to the N terminus of the protein of interest. YFP^N (154 amino acids of YFP and 5-amino acid linker) was amplified with primers fwd_Kpn_YFP-N (5'-CGGTACCATGGTGAGCAAGGGCGAGGAGCTG-3') and rev_YFP-N_Li_Asc (5'-CGGCGCGCCGTGGCGATGGAGCGCAT-GATATAGACGTTGTGGCTGTTGTAG-3'). YFP^C (86 amino acids of YFP and 17-amino acid linker) was amplified with primers fwd_Kpn_YFP-C (5'-CGGTACCATGGCCGACAAGCAGAAGAACGGCATCAAGG-3') and rev_YFP-C_Li_Asc (5'-CGGCGCGCCGTGGTTCATGACCTTCTGTTTCAGG-TCGTTCGGGATCTTGCAGGCCGGGCGCTTGTACAGCTCGTCCATGCCG-AGAGTGATCCC-3'). The KpnI–AscI fragment of YFP^N or YFP^C was li-

gated into KpnI- and AscI-digested pCMB17apx, yielding pDV7 (GFP replaced with YFP^N in pCMB17apx) and pDV8 (GFP replaced with YFP^C in pCMB17apx). To create an N-terminal YFP^C fusion construct of TeaA, the AscI–PacI fragment from pNT1 was subcloned into the corresponding sites of pDV8, yielding pYH02. To produce TeaA N-terminally tagged with YFP^C under the *teaA* native promoter, a 1.5-kb fragment of the *teaA* promoter was amplified from genomic DNA with the primers teaA-pro-EcoRI and teaA-proKpnI, digested with EcoRI and KpnI, and ligated with EcoRI-KpnI–digested pYH02 (*alcA* promoter replaced with the *teaA* promoter in pYH02). Using the same approach, *kipA* and *sepA* fragments from pSK82 (Konzack *et al.*, 2005) and pNT9 were sub-cloned into the corresponding sites of pDV8, yielding pYH05 and pYH14. To create N-terminal YFP^N fusion constructs, *teaA*, *sepA*, and *teaR* fragments from pNT1, pNT9, and pNT7 were subcloned into the corresponding sites of pDV7, yielding pYH01, pYH03, and pYH04.

Table 2. Plasmids used in this study

Plasmid	Construction	Source
pCR2.1-TOPO	Cloning vector	Invitrogen
pENTR/D-TOPO	GATEway TOPO cloning vector	Invitrogen
pCMB17apx	*alcA(p)::GFP*, for N-terminal fusion of GFP to proteins of interest; contains *N. crassa pyr4*	V. Efimov (Piscataway, NJ)
pDM8	GFP replaced mRFP1 in pCMB17apx	Veith *et al.* (2005)
pSK70	*argB* with SfiI sites	Vienken and Fischer (2006)
pI4	*pyroA* from *A. nidulans*	Osmani *et al.* (1999)
pDC1	*argB* from *A. nidulans*	Aramayo *et al.* (1989)
pSK74	1 0.5-kb 5′-flanking region of *teaA* with SfiI site in pCR2.1-TOPO	This study
pSK75	1.0-kb 3′-flanking region of *teaA* with SfiI site in pCR2.1-TOPO	This study
pSK76	*teaA*-deletion construct: flanking regions from pSK74 and pSK75 ligated with *argB* from pSK70	This study
pNRSTE1	1.9-kb *pyr4* with flanking BamHI and NotI sites in pCR2.1-TOPO	Requena *et al.* (2001)
pNT12	1 0.0-kb 5′-flanking region of *teaR* with KpnI and BamHI sites in pCR2.1-TOPO	This study
pNT13	1 0.0-kb 3′-flanking region of *teaR* with NotI and XbaI sites in pCR2.1-TOPO	This study
pNT14	*teaR*-deletion construct: flanking regions from pNT12 and pNT13 ligated with *pyr4* from pNRSTE1	This study
pNT1	0.7-kb *teaA* fragment in pCR2.1-TOPO	This study
pNT5	0.7-kb *teaA* fragment from pNT1 in pCMB17apx	This study
pNT6	0.7-kb *teaA* fragment from pNT1 in pDM8	This study
pNT28	1.5-kb *teaA*(p) fragment in pNT6	This study
pNT7	0.7-kb *teaR* fragment in pCMB17apx	This study
pNT30	1.5-kb *teaR*(p) fragment in pNT7	This study
pNT9	1.2-kb *sepA* fragment in pCMB17apx	This study
pNT16	*TeaR*-ORF without stop-codon in pENTR/D-TOPO	This study
pMT-sGFP	GATEway Vector, *alcA(p)::cccD*-box (incl. *attR*-sites)::*sGFP, argB*	Toews *et al.* (2004)
pNT21	*alcA(p)::teaR-sGFP, argB; teaR* from pNT16 via GATEway in pMT-sGFP	This study
pNT31	*TeaR*-ORF in pCMB17apx	This study
pNT32	*TeaR*-ORF with point mutation at Cys in CAAX motif in pCMB17apx	This study
pDV7	GFP replaced N-terminal half of YFP in pCMB17apx	This study
pDV8	GFP replaced C-terminal half of YFP in pCMB17apx	This study
pYH01	0.7-kb *teaA* fragment from pNT1 in pDV7	This study
pYH02	0.7-kb *teaA* fragment from pNT1 in pDV8	This study
pNT29	1.5-kb *teaA*(p) fragment in pYH02	This study
pYH03	1.2-kb *sepA* fragment from pNT9 in pDV7	This study
pYH04	0.7-kb *teaR* fragment from pNT7 in pDV7	This study
pYH05	1.0-kb *kipA* fragment from pSK82 in pDV8	This study
pYH14	1.2-kb *sepA* fragment from pNT9 in pDV8	This study
pNT33	N-terminal half of *teaA* cDNA in pGADT7	This study
pNT34	N-terminal half of *teaA* cDNA in pGABKT7	This study
pNT35	C-terminal half of *teaA* cDNA in pGADT7	This study
pSH19	C-terminal half of *teaA* cDNA in pGABKT7	This study
pSH10	Full-length of *teaR* cDNA in pGADT7	This study
pSH12	N-terminal half of *sepA* cDNA in pGADT7	This study
pSH14	C-terminal half of *sepA* cDNA in pGADT7	This study

Yeast Two-Hybrid Analysis

The yeast two-hybrid analysis was performed using the MatchMaker3 Gal4 two-hybrid system (Clontech, Mountain View, CA). For bait generation, fragments of *teaA* cDNA corresponding to the N-terminal half of TeaA (1-674 amino acids [aa]) with primers TeaA_EFF (5′-GGCCGAATTCATGGCGTTCCTCTTTA-AATC-3′) and TeaA_BMR (5′-GGCCGGATCCTTAACAAGGCCTCCTGGTGG-3′) or C-terminal half of TeaA (661-1474 aa) with primers TeaA_EMF (5′-GGC-CGAATTCCCTCGCTCACCACGGTT-3′) and TeaA_BRR (5′-GGCCGGATCC-TTAGATCATATTCGCTGCCG-3′) was amplified and cloned in the pGBK7 vector, which contains the GAL4 DNA-BD and the *TRP1* marker, yielding pNT34 and pSH19 (Clontech). The fragments of *teaA* cDNA corresponding to the N-terminal half and C-terminal half of TeaA from pNT34 and pNT19, full-length *teaR* cDNA with primers TeaRF (5′-AAGCAGTGGTATCAACGCA-GAGTGGATGGCGGGTACAGCTACG-3′) and TeaRR (5′-TCTAGAGGC-CGAGGCGGCCGACATGTCACATCACGATGCAGCAT-3′), and fragments of *sepA* cDNA corresponding to the N terminus of SepA (1–700 aa) with primers SepA,N,SMART (5′-AAGCAGTGGTATCAACGCAGAGTGGAT-GCCGACATCCGATAAATCG-3′) and SepA,N,CDS (5′-TCTAGAGGC-CGAGGCGGCCGACATGCCTCCTATCCATAGCCACATA-3′) and fragments of *sepA* cDNA corresponding to the C terminus of SepA (715-1790 aa) with primers SepA,C,SMART (5′-AAGCAGTGGTATCAACGCAGAGTG-GCAGAGCTTGTTAGATCGACTA-3′) and SepA,C,CDS (5′-TCTAGAGGC-

CGAGGCGGCCGACATGAGCACCATCATCGGTATTGTC-3′) were amplified and cloned in the pGADT7 vector, which contains the GAL4 DNA-AD and the *LEU2* marker (Clontech), yielding pNT33, pNT35, pSH10, pSH12, and pSH14. pGBK7 associated plasmids were transformed in yeast Y187 (mating type *MATα*) and pGADT7 associated plasmids were transformed in yeast AH109 (mating type *MAT*a). The system uses two reporter genes (*HIS3* and *LacZ*) under the control of the GAL4-responsive UAS. β-Galactosidase activity was analyzed by liquid culture assay using *o*-nitrophenyl β-ᴅ-galactopyrano-side (ONPG) (Sigma Chemie, Deisenhofen, Germany) as substrate.

Light and Fluorescence Microscopy

For live-cell imaging of germlings and young hyphae, cells were grown on coverslips in 0.5 ml of MM + 2% glycerol (induction of the *alcA* promoter) or MM + 2% glucose (repression of the *alcA* promoter). Cells were incubated at room temperature for 1–2 d. For pictures of young hyphae of each gene deletion strain, the spores were inoculated on microscope slides coated with MM + 2% glucose + 0.8% agarose and grown at 30°C for 1 d. Images were captured at room temperature using an Axiophot microscope (Carl Zeiss, Jena, Germany). Images were collected and analyzed with the AxioVision system (Carl Zeiss).

*N-[3-Triethylammoniumpropyl]-4-
[p-diethylaminophenylhexatrienyl] pyridinium dibromide
(FM4-64), Benomyl, Cytochalasin A, and Filipin
Treatment*

FM4-64 was used at a concentration of 10 μM in the medium. Coverslips were incubated for 5 min and washed. Filipin (Sigma Chemie) was used at a final concentration of 1, 3, 5 μg/ml in medium from a stock solution of 10 mg/ml in methanol. Benomyl, methyl 1-(butylcarbamoyl)-2-benzimidazole carbamate (Aldrich Chemical, Milwaukee, WI), was used at a final concentration of 2.5 μg/ml in medium from a stock solution of 1 mg/ml in ethanol. Cytochalasin A (Sigma Chemie) was used at a final concentration of 2 μg/ml in medium from a stock solution of 100 mg/ml in dimethyl sulfoxide (DMSO).

RESULTS

Isolation of TeaA and TeaR

We searched the *A. nidulans* database for proteins with similarity to the cell end marker protein Tea1 from *S. pombe*, and we identified an open reading frame (AN4564.3) with 27% identity per 1037 amino acids and an e-value of 3e-78 to Tea1. We named the gene *teaA* (Figure 1A). DNA and cDNA sequences were confirmed, and three introns of 88, 58, and 60 base pairs were determined. Although the overall sequence identity is rather low, the architecture of the two proteins is similar. They are 1474 (*A. nidulans*) and 1147 (*S. pombe*) amino acids, and they contain Kelch-repeats in their N-terminal halves and extended coiled-coil regions in their C-terminal halves (determined with http://www.ebi.ac.uk/InterProScan/, http://www.ch.embnet.org/software/COILS_form.html). Sequence identity to the *S. cerevisiae* Kel1 protein is 36% only in the Kelch-repeats. In comparison, orthologues of full-length TeaA are conserved in other filamentous fungi. Because in *S. pombe* a second Kelch-domain protein, Tea3, exists, which has similarity to Tea1 and is associated with the Tea1/Mod5 protein complex (Snaith *et al.*, 2005), we searched the *A. nidulans* database for Tea3 homologues. We found four Kelch-repeat domain-containing proteins, but only TeaA displayed sequence similarity outside the Kelch repeats. This was also the case in other filamentous fungi, besides *A. gossypii*, which contains homologues of Tea1 and of Tea3. However, as Mod5 (see below) demonstrates, it could well be that a functional homologue of Tea3 exists in filamentous fungi but that it displays only low sequence similarity.
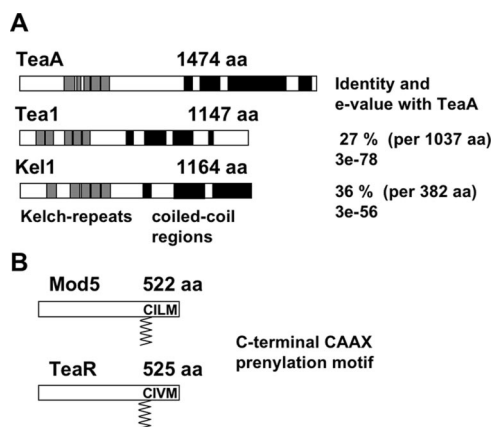

Figure 1. Characterization of TeaA and TeaR. (A) Scheme of *A. nidulans* TeaA, *S. pombe* Tea1, and *S. cerevisiae* Kel1. All three proteins share Kelch-repeats (gray boxes) at the N terminus and extended coiled-coil regions (black boxes) in the C-terminal half of the proteins. (B) Scheme of *A. nidulans* TeaR and *S. pombe* Mod5. The proteins are characterized by a C-terminal CAAX prenylation motif.

Besides Tea1, another crucial cell end marker protein in *S. pombe* is Mod5, which interacts with Tea1 at cell tips and thereby anchors Tea1 along with the formin For3 (Snaith and Sawin, 2003; Martin *et al.*, 2005; Snaith *et al.*, 2005). Despite the important role of Mod5 for polarized growth in *S. pombe*, no sequence homologue was identified in any filamentous fungus. Mod5 is anchored at the membrane through the prenyl residue, which itself is attached to Mod5 via a conserved C-terminal CAAX motif (cysteine, two aliphatic amino acids, any amino acid). Therefore, we anticipated that a functional homologue in *A. nidulans* could also harbor a CAAX motif at the C terminus. We searched the *A. nidulans* database for proteins with such a motif, and we identified 22 candidates. Their sequence identities with Mod5 were below 16%. We selected one (AN4214.3) that showed second highest identity to Mod5 (15.4%), was conserved only in filamentous fungi, and all of those fungal proteins harbored CAAX motifs at their C termini. Because we considered this protein as a putative receptor for TeaA, we named the gene *teaR* (TeaA receptor). DNA and cDNA sequences were confirmed and one intron of 105 base pairs was determined. The TeaR protein consists of 525 amino acids, and it is similar in size to the 522 amino acids of Mod5 (Figure 1B).

Deletion of teaA and teaR

To analyze the function of *teaA* in *A. nidulans*, we constructed a *teaA*-deletion strain (see *Materials and Methods*). The size of the colonies of the Δ*teaA* strain was ~75% compared with that of a wild-type strain (Figure 2A). In the Δ*teaA* strain, the maintenance of growth directionality was altered. Whereas wild-type hyphae normally grow straight, the Δ*teaA* mutant showed zigzag morphology (Figure 2B). A similar effect was shown for the kinesin motor mutant Δ*kipA* (Konzack *et al.*, 2005). The Δ*kipA* mutant displayed curved hyphae, which are similar but not identical to the Δ*teaA*-mutant hyphae (Figure 2B). It has been revealed that the Spitzenkörper, whose position is associated with growth direction, often moved away from the center of the hyphal apex in the Δ*kipA* mutant, and the hyphae grew in the direction of the Spitzenkörper. In the Δ*teaA* hyphae, the Spitzenkörper often mislocalized and moved away from the center to one side in the hyphal apex (data not shown). The curved hyphae in the Δ*kipA* mutant and the zigzag hyphae in the Δ*teaA* mutant were most prominent in younger hyphae. In particular, most hyphae at the edge of a larger colony of the Δ*kipA* mutant looked normal, and the Δ*kipA* mutant did not show growth delay. Conversely, mature hyphae in the Δ*teaA* mutant showed hyperbranching, and colonies grew slower than wild type or the Δ*kipA* strain.

In the Δ*kipA* mutant, another polarity defect has been detected in the way the second germ tube emerges from a conidiospore. In wild type, the second hypha emerges from the side of the spore opposite to the germ tube (bipolar) in 73% of the spores (Figure 2C; n = 200). In contrast, the second hyphae emerged in random positions in 80% of the spores in the Δ*kipA* mutant. A similar defect was observed in 58% of the spores in the Δ*teaA* mutant. This shows that TeaA also determines the initiation of polarity.

To explore the function of *teaR*, we constructed a *teaR*-deletion strain (see *Materials and Methods*). The Δ*teaR* mutant also showed the defect in the maintenance of growth directionality, and it displayed curved hyphae, which was identical to the Δ*kipA* mutant (Figure 2B), suggesting that TeaR functions in the same pathway as KipA. Likewise, the curved hyphae in the Δ*teaR* mutant were prominent in young hyphae, but they were not observed at the edge of a mature colony. Hence, the Δ*teaR* mutant did not show a
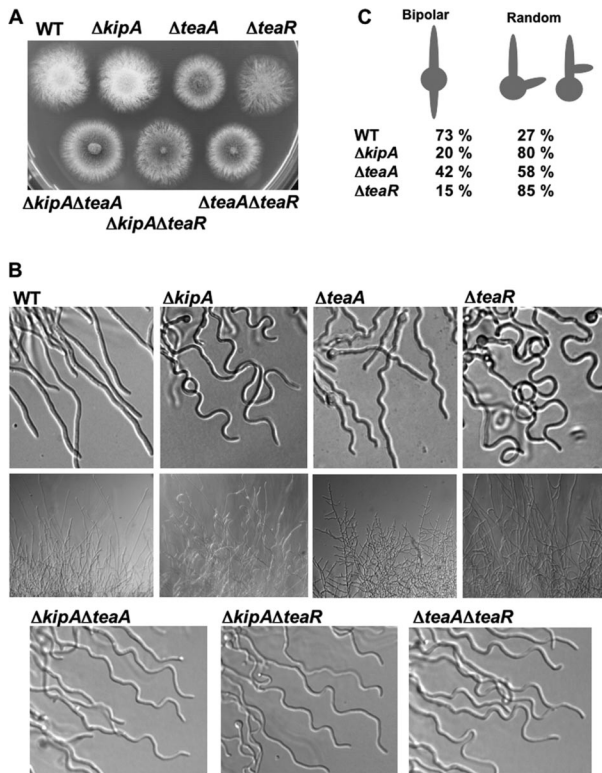
Figure 2. Phenotypic comparison of Δ*kipA*, Δ*teaA*, Δ*teaR*, and corresponding double mutants. (A) Colonies of wild type (GR5), Δ*kipA* (SRL1), Δ*teaA* (SSK91), Δ*teaR* (SNT33), Δ*kipA*/Δ*teaA* (SNT14), Δ*kipA*/Δ*teaR* (SNT40), and Δ*teaA*/Δ*teaR* (SNT39) strains. Strains were grown on minimal medium glucose agar plates for 2 d. (B) Differential interference contrast images of wild type, Δ*kipA*, Δ*teaA*, Δ*teaR*, Δ*kipA*/Δ*teaA*, Δ*kipA*/Δ*teaR*, and Δ*teaA*/Δ*teaR* strains as indicated. Strains were grown on microscope slides coated with minimal medium, with glucose and 0.8% agarose for 1 d (top and bottom). Strains were grown on minimal medium glucose agar plates for 2 d (middle). Hyphae are 3–4 μm in diameter. (C) Quantification of the effect of the gene deletions on second germ tube formation. Conidia of each strain were germinated in minimal medium with glucose, and then they were analyzed for the emergence of the second germ tube. For each strain, 200 germlings were counted.

growth delay when colony diameters were compared (Figure 2A). When we determined the site of the second hypha formation from a spore, we found random emergence in 85% of the spores in the Δ*teaR* mutant (Figure 2C).

To analyze the genetic interaction of *kipA*, *teaA*, and *teaR*, corresponding double-deletion strains were constructed by crossing. All three strains showed a curved hyphal phenotype (Figure 2B), which was identical to those in the Δ*kipA* and the Δ*teaR* mutant. The Δ*kipA*/Δ*teaA* mutant and Δ*teaA*/Δ*teaR* mutant showed a slight growth defect, although their colonies were bigger than that of the Δ*teaA* single mutant (Figure 2A), and they did not show a significant increase in branching. The Δ*kipA*/Δ*teaR* mutant showed no additional phenotype in comparison to the single mutants. All single mutants showed defects in growth directionality and only the Δ*teaA* mutant showed a growth defect. Genetic analysis indicated that deletion of *kipA* or *teaR* could partially suppress the growth defect of the Δ*teaA* mutant but not the maintenance of growth directionality.

Localization of TeaA and TeaR

To investigate TeaA localization, we constructed an *A. nidulans* strain expressing a GFP-TeaA fusion protein under the control of the regulatable *alcA* promoter (see *Materials and Methods*). Under repressing conditions, the strain, in which GFP-TeaA is the only source of TeaA, showed the zigzag hyphal phenotype observed in the Δ*teaA* mutant (data not shown), whereas the phenotype was restored under derepressed conditions, proving that GFP-TeaA is biologically functional. Using the same approach, we confirmed that mRFP1-TeaA was also biologically functional, and thus GFP or mRFP1 tagging did not show any difference. Under derepressed conditions, GFP-TeaA localized to one point at all hyphal tips (Figure 3A). The GFP-TeaA points always attached or localized quite close to the plasma membrane. GFP-TeaA detached from the cortex was not observed. A single GFP-TeaA spot was also observed in conidiospores before germination (bottom left). Some GFP signal spots,
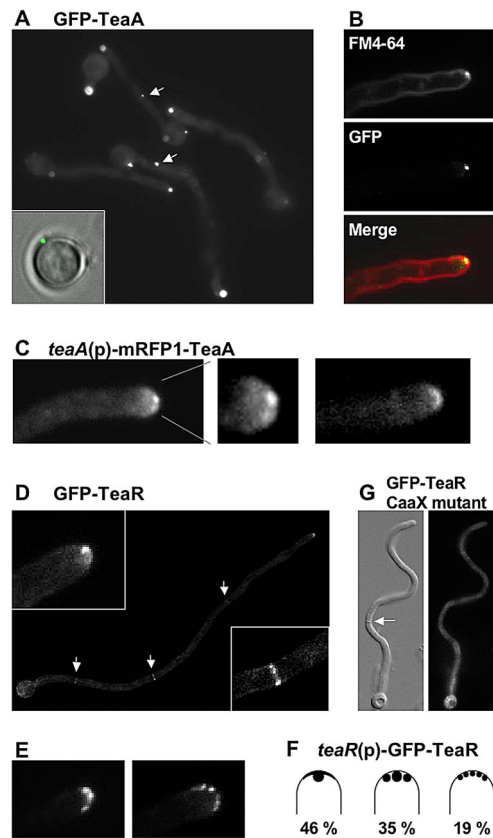

Figure 3. TeaA and TeaR localization. Strains SNT4 (A and B), SNT49 (C), SNT26 (D, E), SNT55 (F), and SNT61 (G) were grown on minimal medium with glycerol as carbon source. (A) GFP-TeaA localized to one point in the apex of all hyphal tips and some points in the cell body (arrows). The TeaA spot showed up in conidia before germination (left bottom). (B) The membrane was stained with FM4-64 (top, red in merged image). The Spitzenkörper labeled by FM4-64 colocalized with GFP-TeaA point (middle, green in merged image) at the tip. (C) mRFP1-TeaA produced under native promoter control localized to one point at most of tips and weaker signals were observed along the tip membrane. (D) GFP-TeaR localized to one point at hyphal tips and along the apex (left inset) and septa (arrows, right inset). (E) GFP-TeaR localized to one main point and two smaller points next to the main point at hyphal tips (left). GFP-TeaR spots aligned along the apex (right). (F) The percentage of GFP-TeaR localization pattern; 100 hyphal tips were analyzed. Hyphae are 3–4 μm in diameter.

Table 3. Localization pattern of mRFP1-TeaA

teaA(p)-mRFP1-TeaA					
WT[a]	80	7	0	13	0
WT with benomyl[b]	2	3	10	2	83
Δ*kipA*[c]	43	35	8	14	0
KipA-rigor[d]	30	34	15	9	10
cytochalasin A[e]	56	6	6	9	23

The localization pattern of 100–200 hyphal tips was analyzed and grouped into five different categories. The numbers indicate the percentage of hyphal tips of these groups.

SNT49 (a), SNT50 (c), and SNT51 (d) were grown on minimal medium with glycerol for 1 day. SNT49 (b) and SNT57 (e) were grown under the same conditions as above and treated with 2.5 μg/ml benomyl (b) or 2 μg/ml cytochalasin A (e) for 30 min. mRFP1-TeaA localization was analyzed within 10 min.

which were weaker compared with the point at the hyphal apex, were observed in the hyphal body (arrows). To compare the localization of TeaA and the Spitzenkörper, we stained hyphae with FM4-64. This compound has been used in several fungi to stain the Spitzenkörper (Fischer-Parton *et al.*, 2000; Peñalva, 2005). The Spitzenkörper labeled by FM4-64 colocalized with GFP-TeaA at the hyphal apex (Figure 3B), although the Spitzenkörper was labeled only in a small number of tips under our experimental conditions. To confirm the TeaA localization, we constructed strains producing mRFP1-TeaA under the control of the native promoter. A strain, in which mRFP1-TeaA is the only source of TeaA, did not show the phenotype observed in the Δ*teaA* mutant, indicating that mRFP1-TeaA also was biologically functional. Although signals of mRFP1 seemed weaker, mRFP1-TeaA still localized to one point at most of the tips, and weaker signals were observed along the apex (Figure 3C, left). The single spot of mRFP1-TeaA normally localized at the center of the hyphal apex (Table 3). At a small number of tips, mRFP1-TeaA localized along the tip membrane but not to one point (Figure 3C, right, and Table 3). Hereafter, we normally used strains producing mRFP1-TeaA under the native promoter, when we analyzed the localization of TeaA.

Using the same approach as for TeaA, we constructed a strain producing GFP-TeaR under *alcA* promoter control (see *Materials and Methods*). Under repressing conditions, the strain showed curved hyphae as observed in the Δ*teaR* mutant (data not shown). In contrast, under derepressing conditions, the curved hyphal phenotype was restored, indicating that GFP-TeaR is functional. GFP-TeaR localized to hyphal tips and all septa (Figure 3D). GFP-TeaR localized to one point at most of the tips, and weaker signals were observed along the apex, similar to the localization of TeaA. The GFP-TeaR point also colocalized with the Spitzenkörper labeled by FM4-64 (data not shown). Sometimes, one or two smaller GFP-TeaR spots localized close to a larger point (Figure 3E). At <20% of the tips, GFP-TeaR spots aligned along the apex, but they did not localize uniform along the cortex. To study the localization of TeaR under native conditions, we constructed strains producing GFP-TeaR under *teaR* promoter control. The strains did not show the phenotype of a Δ*teaR* mutant, indicating the functionality of the GFP-TeaR fusion protein. The localization of GFP-TeaR was identical to that in of the *alcA* promoter (Figure 3F). There-

fore, we used strains producing GFP-TeaR under *alcA* promoter control, when we analyzed the localization of TeaR. In addition, it seems that TeaR localizes to septa; however, we did not observe any alteration in septation in *teaR*-deletion strains (data not shown).

TeaR is assumed to localize to the plasma membrane through its prenyl residue. The nonuniform spot-like localization of TeaR at the apex may reflect sterol-rich membrane microdomains (see below). To prove the importance of the C-terminal CAAX motif in TeaR, we constructed a strain, producing TeaR (GFP tag at the N terminus) where the cysteine residue in the CAAX motif was changed to glycine by point mutation. The mutated GFP-TeaR could not rescue the phenotype of the Δ*teaR* mutant, and only weak GFP fluorescence was observed throughout the hyphae (Figure 3G), whereas GFP-tagged wild-type TeaR could rescue the phenotype of the Δ*teaR* mutant, and it localized to tips and septa (data not shown). Likewise, TeaR tagged with GFP at the C terminus, and thus masking the CAAX motif, failed to rescue the phenotype of the Δ*teaR* mutant, and it did not localize to tips and septa (data not shown). These results demonstrate that the C-terminal CAAX motif is necessary for TeaR localization and function.

Role of TeaA in Microtubule Organization at Hyphal Tips

To analyze the role of TeaA at hyphal tips, we investigated the relationship of TeaA and MTs. In wild type, MTs elongate toward the apex, reach the tip cortex, and normally converge in one point at the center of the tip. To compare the localization of TeaA and the convergence point of MTs, we constructed a strain expressing GFP-labeled α-tubulin and mRFP1-TeaA. We found that the point where GFP-MTs converged colocalized with the mRFP1-TeaA spot (Figure 4A and Supplemental Movie 1).

In *S. pombe*, Tea1 is delivered by growing MTs to the cell tip, and its localization at the cell tips depends on MTs. Whereas in *A. nidulans* KipA showed the same behavior as Tea1 in *S. pombe*, we have no evidence that TeaA accumulates at the MT plus ends. To test whether TeaA localization at tips nevertheless depends on MTs, we used the MT-destabilizing drug benomyl. After this treatment (2.5 μg benomyl/ml), almost all fluorescence of GFP-MTs was diffused into the cytoplasm within 5 min (data not shown), and the mRFP1-TeaA point at the tips was sometimes divided into several points and disappeared from >80% of the tips after 30–40 min (Figure 4B and Table 3; n = 100). Control treatment with 0.25% ethanol did not show the effect on the localization of mRFP1-TeaA. These results indicated that TeaA localization at tips depends on MTs.

To study the behavior of MTs in a Δ*teaA* mutant, we compared wild type and Δ*teaA* strains expressing GFP-labeled α-tubulin. These strains did not show apparent differences in the number of MTs in the cytoplasm. In the tip of wild type, MTs elongated toward the apex and normally converge in one point at the center of the tip (>80% of tips during 1-min observation), and they paused there without elongating until a catastrophe event caused depolymerization. In the Δ*teaA* mutant, MTs reached the tip cortex, but sometimes they did not converge to one, but attached to several points. The phenomenon was observed at 45 tips (n = 100) during 1-min observation (Figure 4, C and E, and Supplemental Movie 2). Moreover, MTs in the Δ*teaA* mutant seemed more curved than those of wild type, and a few MTs bent around the tips. The bending of MTs could be due to continuous elongation after they reached the cortex. Bending of MTs was observed in 22 tips (n = 100) during 1-min observation in the Δ*teaA* mutant, whereas it was observed in
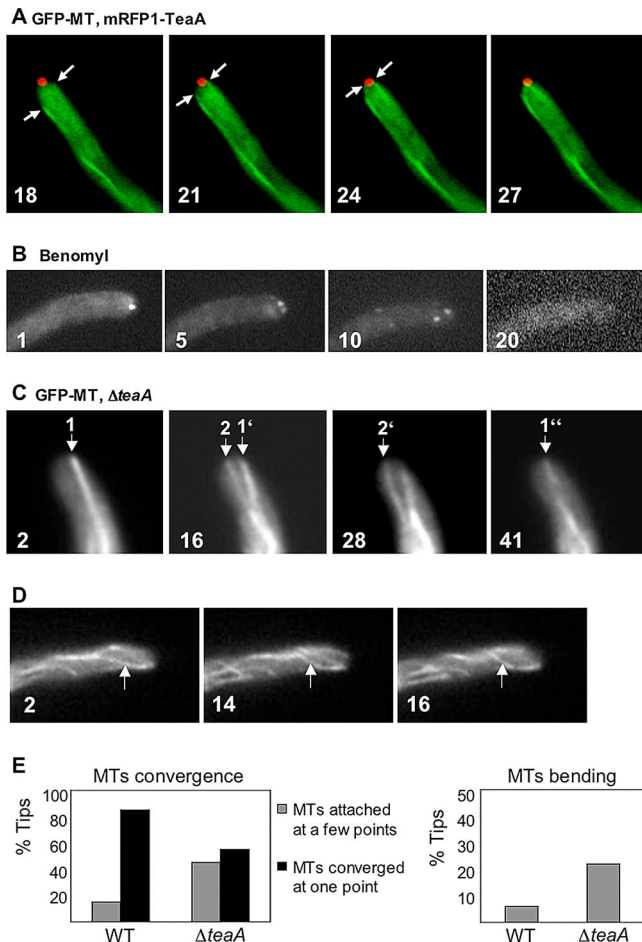
A GFP-MT, mRFP1-TeaA

B Benomyl

C GFP-MT, Δ*teaA*

D

E

MTs convergence

MTs bending

□ MTs attached at a few points

■ MTs converged at one point

Figure 4. Relationship between TeaA and microtubules (MT). (A) In strain SNT22 (GFP-MT, mRFP1-TeaA), GFP-MTs elongated toward the hyphal tip (arrow) and merged at one point at the apex. The point colocalized with mRFP1-TeaA point at the apex (see Supplemental Movie 1). Times are indicated in seconds. (B) SNT49 [*teaA*(p)-mRFP1-TeaA] was grown in minimal medium with glycerol for 1 d and treated with the medium containing 2.5 μg/ml benomyl. mRFP1-TeaA point at tips was sometimes divided into a few points and disappeared from >80% of tips after 30 min (see Table 3). Elapsed time is given in minutes. (C) In strain SNT 31 (Δ*teaA*, GFP-MT), GFP-MTs did not merge in one point at the apex but instead attached to a few points (arrows indicate points where MT attached; see Supplemental Movie 2). Elapsed time is given in seconds. (D) In the strain SNT 31, GFP-MTs became more curved than those in wild type. GFP-MTs bent, probably because they kept growing after they reached the cortex (arrows; see Supplemental Movie 3). Elapsed time is given in seconds. Hyphae are 3–4 μm in diameter. (E) Quantification of MTs behavior in SNT22 (GFP-MT, mRFP1-TeaA) and SNT31 (Δ*teaA*, GFP-MT). The percentage of tips where GFP-MTs merged in one point (black bar) or attached to a few points (gray bar) (left), and the percentage of tips where GFP-MTs bent after they attached to the cortex (right). Data from 100 tips of strain SNT22 and SNT31 during 1-min observation.

six tips (n = 100) during 1-min observation in wild type (Figure 4, D and E, and Supplemental Movie 3).

Relationship between KipA and TeaA

In *S. pombe*, Tea1 is transported by the kinesin Tea2 along MT to the plus end, where both proteins accumulate. This leads to comet-like structures in time-lapse observations (Busch *et al.*, 2004). To test whether *A. nidulans* TeaA is
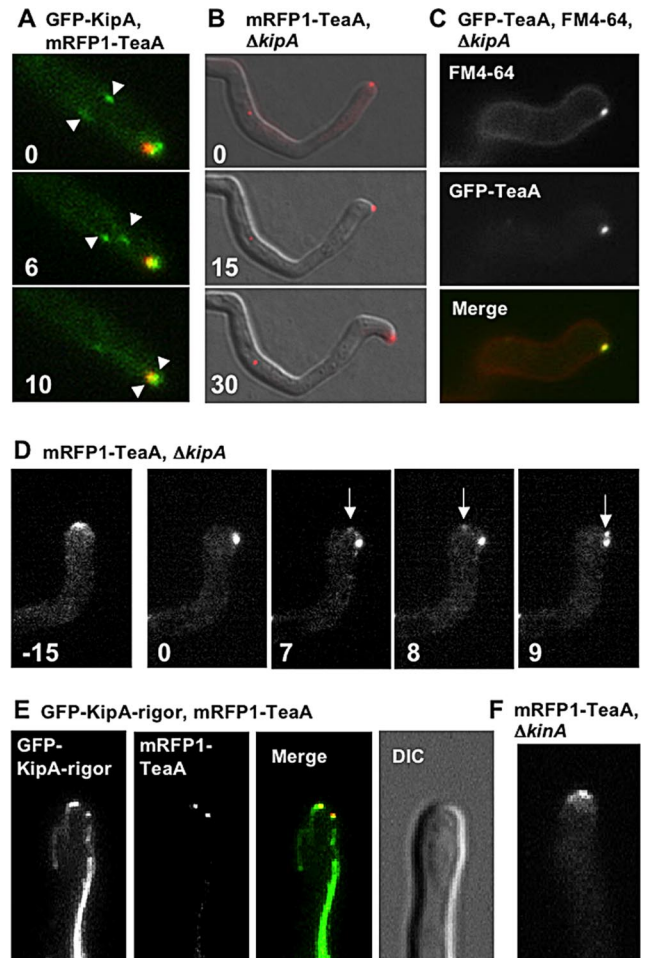

A GFP-KipA, mRFP1-TeaA

B mRFP1-TeaA, Δ*kipA*

C GFP-TeaA, FM4-64, Δ*kipA*

FM4-64

GFP-TeaA

Merge

D mRFP1-TeaA, Δ*kipA*

E GFP-KipA-rigor, mRFP1-TeaA

GFP-KipA-rigor

mRFP1-TeaA

Merge

DIC

F mRFP1-TeaA, Δ*kinA*

Figure 5. Relationship between TeaA and KipA. (A) In strain SNT23 (GFP-KipA, mRFP1-TeaA), GFP-KipA spots, which label MT plus ends, moved toward the hyphal tip (arrows), and they merged at one point at the apex with mRFP1-TeaA (see Supplemental Movie 4). Elapsed time is given in seconds. (B and C) In the Δ*kipA* mutant (SNT41), mRFP1-TeaA still localized to one point at the hyphal tip but often moved away from the center of the apex (see Table 3). Elapsed time is given in minutes. (C) In the Δ*kipA* mutant (SNT9), the Spitzenkörper labeled by FM4-64 (top, red in merged image) also moved away from the center of the apex and colocalized with the GFP-TeaA point at the tips (middle, green in merged image). (D) In the Δ*kipA* mutant (SNT50), mRFP1-TeaA moved away from the center of the apex to the side of the tip, and it divided into two points (arrows; see Supplemental Movie 5). Elapsed time is given in minutes. (E) In the *kipA*-rigor mutant (SNT51), mRFP1-TeaA sometimes localized to two points at the tip (see Table 3), whereas GFP-KipA^{G223E} decorated MTs and MTs attached to the two points. (F) Deletion of *kinA* did not affect mRFP1-TeaA tip localization (strain SNT62). Hyphae are 3–4 μm in diameter.

transported by KipA, the Tea2 orthologue, we compared TeaA and KipA localization. The GFP-KipA signal accumulated at MT plus ends, moved toward the tip, and converged to the mRFP1-TeaA point at the apex (Figure 5A and Supplemental Movie 4). In contrast, TeaA was not detected at MT plus ends. This could be explained if TeaA uses a different mechanism to reach the cell tip or if TeaA accumulates at the MT plus end only to very low concentrations, below the detection level of mRFP1. To test the second possibility, we analyzed TeaA localization in a Δ*kipA* mutant. GFP- or mRFP1-tagged TeaA still localized to one point
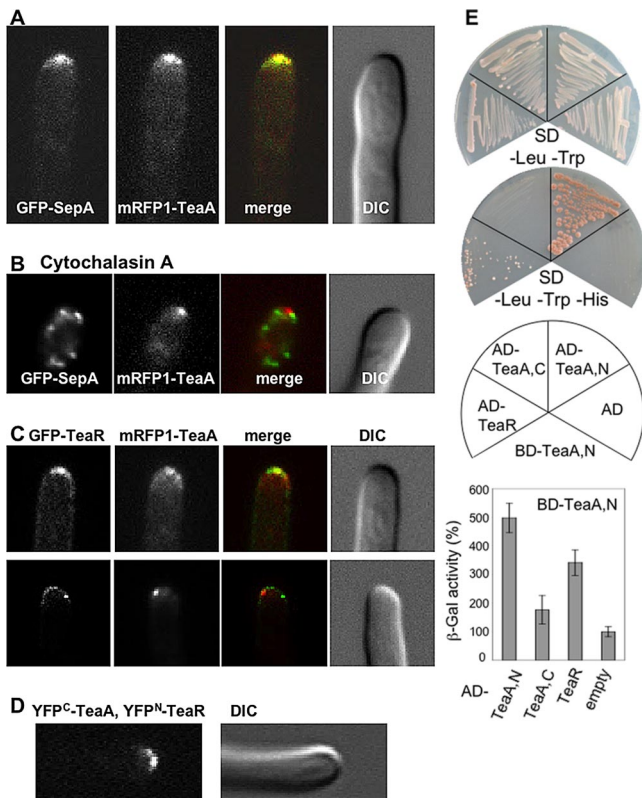
Figure 6. Interaction of TeaA, SepA and TeaA, TeaR. (A) GFP-SepA and mRFP1-TeaA colocalized to one point at the apex and along the apex in strain SNT57. (B) Strain SNT57 grown in minimal medium with glycerol for 1 d was treated with the medium containing 2 μg/ml cytochalasin A for 30 min. (C) In strain SNT56, the mRFP1-TeaA point at the apex colocalized with that of GFP-TeaR, although their localization was not identical. (D) BiFC analysis of TeaA and TeaR. In SNT59 expressing TeaR tagged with the N-terminal half of YFP and TeaA tagged with the C-terminal half of YFP, the YFP signal was detected at the tip. (E) Yeast two-hybrid interaction between the DNA binding domain fused to the TeaA N-terminal half (BD-TeaA,N) and the activation domain fused to the TeaA N- or C-terminal half (AD-TeaA,N, AD-TeaA,C), TeaR full length (AD-TeaR), or as control the empty vector (AD). The mated yeasts were selected on SD/−Leu/−Trp plate (top) and grown on nutritionally selective plate SD/−Leu/−Trp/-His (bottom). β-Galactosidase activity was analyzed by liquid culture assay using ONPG as substrate. The value of BD-TeaA,N and AD was used as a standard (100%). The data are expressed as the mean ± SD (n = 4).

at ~80% of tips, but often it did not localize to the center of the apex (Figures 5B and 7A and Supplemental Table 3). When the mRFP1-TeaA point moved away from the center of the apex to right or left side of the apex, hyphae grew in the direction of the TeaA location (Figure 5B). This result suggests that TeaA localization is involved in the determination of growth direction and that the Δ*kipA* mutant displays meandering hyphae possibly partly due to mislocalization of TeaA at tips. The Spitzenkörper labeled by FM4-64 also often mislocalized and colocalized with TeaA at the tips (Figure 5C). Besides mislocalization of TeaA to a side of the cortex at the tips, TeaA occurred as two points at <10% of the tips (Figure 5D and Table 3). The TeaA point moved along the tip cortex and divided into two points (Figure 5D and Supplemental Movie 5). To analyze further the role of KipA for TeaA localization, we checked TeaA localization in a *kipA*-rigor mutant, in which KipA harbors a point muta-

tion in the ATP-binding domain (P-loop, G223E). The mutated GFP-KipA-rigor binds but does not move along MTs; thus, it decorates them (Konzack *et al.*, 2005). In the *kipA*-rigor mutant, mRFP1-TeaA still localized at 90% of the tips, but the mRFP1-TeaA point often moved away to the side of the apex and sometimes divided into two points (Table 3). These results indicate that TeaA accumulation at tips is independent of KipA, but KipA is necessary for proper TeaA anchorage at the tips. MTs visualized by GFP-KipA-rigor elongated to tips and attached to mRFP1-TeaA even if it localized to a point at the side of the apex or if mRFP1-TeaA was split into two points (Figure 5E). This supported the idea that TeaA is necessary for proper MT organization in the tip.

Because conventional kinesin has been reported to transport dynein toward the MT plus end (Zhang *et al.*, 2003), we analyzed TeaA localization in a conventional kinesin *kinA*-deletion strain, but we found no difference to TeaA localization in wild type (Figure 5F).

Interaction of TeaA and SepA

One of the important functions of Tea1 in *S. pombe* is the contribution to cell polarity and actin cable organization through interaction with the formin For3 (Feierbach *et al.*, 2004). Tea4, which was identified as Tea1-interacting protein, binds Tea1 and For3 directly and links Tea1 with For3 (Martin *et al.*, 2004). Therefore, we investigated whether *A. nidulans* TeaA colocalized with the formin SepA. We constructed a strain expressing GFP-SepA and mRFP1-TeaA, and we found colocalization in one point and along the apex (Figure 6A). Direct interaction of TeaA and SepA was tested with the yeast two-hybrid system, but no interaction was detected (data not shown).

It has been shown that SepA localization at hyphal tips depends on the actin cytoskeleton (Sharpless and Harris, 2002). After treatment with 2 μg/ml cytochalasin A, an inhibitor of actin polymerization, GFP-SepA points dispersed around the tips within 10 min (Figure 6B). In contrast, mRFP1-TeaA localization was partially affected by the drug but remained concentrated at >70% of the tips after the 30- to 40-min treatment (Figure 6B and Table 3). We confirmed that the control treatment with 0.02% DMSO did not show the effect on the localization of TeaA and SepA. These observations suggest that TeaA can localize to the tips independently of SepA and independently of an intact actin cytoskeleton.

Interaction of TeaA and TeaR

To investigate whether TeaR functions as a TeaA receptor, we constructed a strain expressing mRFP1-TeaA and GFP-TeaR, and we compared their localization. The mRFP1-TeaA point at the apex colocalized with that of GFP-TeaR at >80% of the tips, although their localization was not identical. GFP-TeaR was restricted to the tip membrane, whereas mRFP1-TeaA was observed at the membrane, and as a gradient away from the membrane (Figures 3C and 6C, top). When GFP-TeaR was observed as some spots along the membrane (Figure 3E, left), the mRFP1-TeaA point colocalized with one of the GFP-TeaR spots, but it did not accumulate at additional points (data not shown). At a few tips, several GFP-TeaR spots aligned along the apex, whereas only one mRFP1-TeaA point was visible (Figure 6C, bottom).

Colocalization of TeaA and TeaR was confirmed by BiFC analysis. The YFP[N] was fused to TeaR, and the YFP[C] was tagged with TeaA. In the strain expressing only YFP[N]-TeaR or YFP[C]-TeaA, no YFP fluorescence was detected. In con-
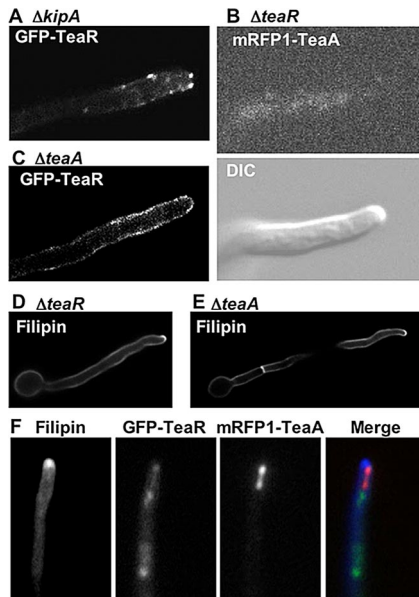
Figure 7. Localization dependency of KipA, TeaA, TeaR, and sterol-rich regions. (A) In the Δ*kipA* mutant (SNT43), some GFP-TeaR signal localized at the membrane of the apex, and other signal dispersed along the membrane away from the tip. (B) In the Δ*teaR* mutant (SNT53), mRFP1-TeaA was not observed at the tip. (C) In the Δ*teaA* mutant (SNT32), GFP-TeaR lost the preference for the hyphal tip and diffused all along the membrane. (D and E) The Δ*teaR* (SNT33) and Δ*teaA* (SSK91) mutants were stained with 10 μg/ml filipin for 5 min. (F) Strain SNT27 was treated with 10 μg/ml filipin for 5 min. Filipin accumulated at the tip (blue in merged image), GFP-TeaR lost the membrane association (green in merged image), and mRFP1-TeaA dispersed at the tip (red in merged image). Hyphae are 3–4 μm in diameter.

trast, in the strain expressing both YFP[N]-TeaR and YFP[C]-TeaA, YFP signals were detected as a single point and along the apex (Figure 6D). The localization pattern of the YFP signal was similar to that of GFP-TeaR. Together, the results suggest that some TeaA colocalizes with TeaR at the apex but that additional TeaA localizes to the tips independently of TeaR.

The protein-protein interaction between TeaA and TeaR was analyzed with the yeast two-hybrid system. Direct interaction between the TeaA N-terminal half and TeaR was detected, although it was weak (Figure 6E). Moreover, self-interaction of the N-terminal halves of TeaA was discovered.

We also checked possible interactions of KipA and TeaA, KipA and TeaR, KipA and SepA, and TeaR and SepA by the BiFC system, but none of these combinations resulted in YFP fluorescence (data not shown). The combination of TeaA with SepA gave a positive YFP signal, but an interaction could not be verified with the yeast two-hybrid assay.

Localization Dependency of KipA, TeaA, and TeaR

As mentioned above, in the Δ*kipA* mutant GFP-TeaA still localized to hyphal tips but often moved away from the center of the apex (Figure 5, B–D, and Table 3). Next, we studied the effect of *kipA*-deletion on TeaR localization. In wild type, TeaR were concentrated in the Spitzenkörper or some spots of TeaR aligned along the membrane at the apex (Figure 3, D and E), whereas in the Δ*kipA* mutant, some GFP-TeaR dots remained at the apex, but in addition, other dots moved to the subapical membrane (Figure 7A, within

10 μm from the tip). These results indicated that KipA is required for TeaR anchorage and proper TeaA positioning.

To determine whether TeaR is involved in TeaA localization, we investigated TeaA localization in a Δ*teaR* mutant. Fluorescence of mRFP1-TeaA was not observed at hyphal tips (Figure 7B). These results indicate that TeaR is required for TeaA anchorage. In contrast, we analyzed the localization of TeaR in a Δ*teaA* mutant and found that GFP-TeaR spread away from hyphal tips (Figure 7C), indicating that TeaA is also required for TeaR anchorage. These results show that TeaA and TeaR localizations are interdependent.

Localization Dependency of TeaA, TeaR, and Sterol-rich Membrane Domains

TeaR is assumed to localize to the membrane through its prenyl residue; therefore, it could be that the membrane environment is important for TeaR localization. In other eukaryotes such membrane microdomains are important for cell signaling, polarity, and protein sorting (Rajendran and Simons, 2005). In fungi, sterol-rich plasma membrane domains were observed by sterol-binding fluorescent dye filipin staining at tips of mating projections in *S. cerevisiae* (Bagnat and Simons, 2002) and *Cryptococcus neoformans* (Nichols *et al.*, 2004), at cell ends and septa in *S. pombe* (Wachtler *et al.*, 2003), and at hyphal tips and septa in *C. albicans* hyphae (Martin and Konopka, 2004). In *A. nidulans*, filipin stained the hyphal tip membrane and septa (Pearson *et al.*, 2004). In Δ*kipA*, Δ*teaA*, and Δ*teaR* strain, filipin stained the hyphal tip and septa identical to wild type (Figure 7, D and E; data not shown). Incubation of cells in high filipin concentrations, for longer times, or both has been demonstrated to alter the sterol-containing membranes and disrupt their functions (Rothberg *et al.*, 1990; Wachtler *et al.*, 2003). Therefore, we analyzed the localization of mRFP1-TeaA and GFP-TeaR under high concentrations of filipin (10 μg/ml; 5 min), and we found that GFP-TeaR was shifted from the membrane at the apex to the cytoplasm or internal membranes (Figure 7F). Filipin treatment changed also slightly the mRFP1-TeaA localization, which resembled the one in the absence of TeaR. The YFP signal from YFP[N]-TeaR and YFP[C]-TeaA also disappeared from the apex after filipin treatment (data not shown).

To investigate the effect of filipin on hyphal growth and on the localization of TeaA and TeaR in more detail, we observed the hyphal morphology under conditions with different filipin concentrations. With <1 μg/ml filipin, hyphae grew normally. Increasing filipin concentrations abolished hyphal growth, and with 5 μg/ml filipin germination was completely inhibited (Figure 8A). The control treatment with 0.05% of methanol did not show the effect. In the presence of 3–4 μg/ml filipin, abnormal hyphal morphologies were often observed (Figure 8B). Next, we investigated the effect of different filipin concentrations on the localization of TeaA and TeaR. To compare the sensitivity of TeaA and TeaR toward filipin treatment, we studied the localization of the proteins at 1, 3, or 5 μg/ml filipin (Figure 8C). Treatment with 1 μg/ml filipin for 1 h had little effect on the localization, whereas 3 μg/ml filipin caused mRFP1-TeaA and GFP-TeaR disappearance at 80% of the hyphal tips. Immediately after the treatment of 3 μg/ml filipin, filipin stained almost all the apex and the signal intensity became gradually stronger (Figure 8D). Although GFP-TeaR often moved away from the apex to subapical membrane regions immediately, mRFP1-TeaA could stay at tips for several minutes and then start to disperse around tips and finally disappear. These results suggest that filipin treatment disrupts TeaR localization and indirectly affects TeaA localization. However, the hyphae treated with filipin did not show the
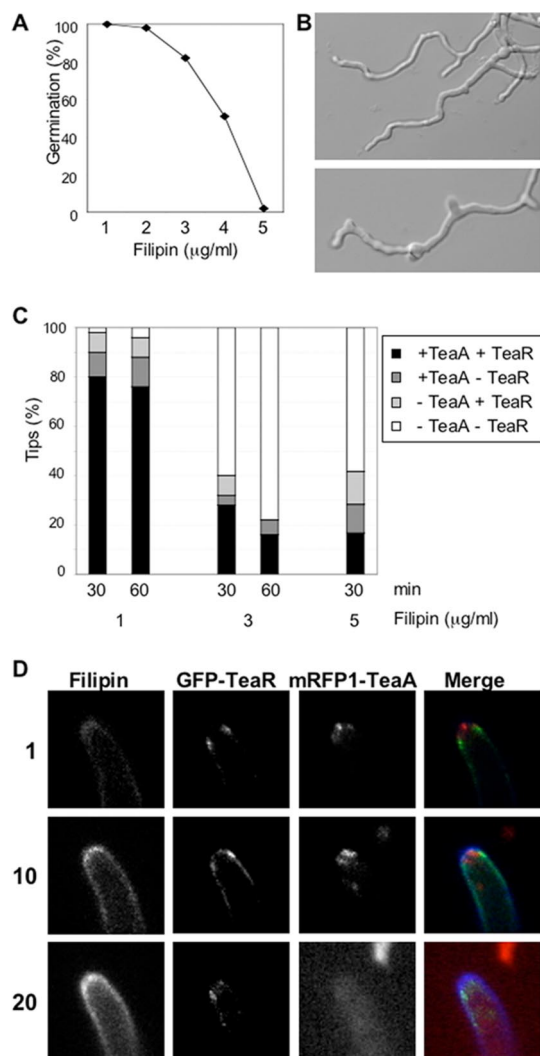
Figure 8. Effect of filipin treatment on hyphal growth and localization of TeaA and TeaR. (A) Germination efficiency. Conidia of wild type (GR5) were inoculated in minimal medium with glycerol in the presence of 1–5 µg/ml filipin, incubated for 36 h, and analyzed for germ tube emergence. Two hundred germlings or conidia were counted. (B) Differential interference contrast images of wild type grown in minimal medium with glycerol and 3 µg/ml filipin for 36 h. (C) Quantification of the number of tips where mRFP1-TeaA and GFP-TeaR localized correctly or not at the tip membrane. Strain SNT56 grown in minimal medium with glycerol for 24 h was treated with the medium containing 1, 3, or 5 µg/ml filipin for 30 or 60 min. Percentage of the tips with the correct localization of mRFP1-TeaA and GFP-TeaR (black bar), with only mRFP1-TeaA (dark gray bar), with only GFP-TeaR (bright gray bar), and without both (white bar); 100 tips were counted. (D) Time course illustration of the localization patterns after the treatment with 3 µg/ml filipin quantified in C. Elapsed time is given in minutes. Hyphae are 3–4 µm in diameter.

same hyphal morphology as Δ*teaA* or Δ*teaR* mutants. This suggests that filipin treatment disrupts not only TeaA and TeaR localization and function but also other polarity factors.

DISCUSSION

Polarized growth is essential in many elongated cells, such as neurites, pollen tubes, or filamentous fungi (Nelson,

2003). Three main structures have been described in fungi to be important for the establishment and maintenance of polarity: the polarisome, cell end factors or landmark proteins, and the Spitzenkörper. Whereas landmark proteins of *S. cerevisiae* seem largely not to be conserved in filamentous fungi (Harris and Momany, 2004; Wendland and Walther, 2006), we show here that the functions of *S. pombe* cell end markers seem to be conserved. However, it has to be noted that also *S. cerevisiae* polarity factors—besides the components of the polarisome—can be used for filamentous growth, for example, in *A. gossypii* (Wendland, 2003; Philippsen *et al.*, 2005). Although the genomes of the two fungi are very similar and reflect a common history, the growth modes are very different, budding in the one and obligatory filamentously in the other species (Dietrich *et al.*, 2004).

The detailed study of TeaA and TeaR in this article revealed that main players of polarity establishment of *S. pombe* are conserved in *A. nidulans* but also that significant differences exist. For example, in *S. pombe* Tea1 is transported by Tea2 toward the MT plus end, with which it hitchhikes through the cell to arrive at the growing tip, whereas in *A. nidulans* we do not have any evidence for such a transport mechanisms. TeaA tip localization was independent of the Tea2 homologue KipA, although it was affected by an MT-depolymerizing drug. Likewise, lack of KipA only slightly affected MT plus-end localization of ClipA, the Clip-170 homologue in *A. nidulans*, at elevated temperature (Efimov *et al.*, 2006), whereas MT plus-end localization of Tip1, the Clip-170 homologue in *S. pombe*, strictly depended on Tea2 (Busch *et al.*, 2004). Nevertheless, we found that KipA is important for proper localization of TeaA and also TeaR in *A. nidulans*. Deletion of *teaR* prevents the formation of a discrete, spot-like structure of TeaA in the tip, and *kipA* deletion allows the formation of the spot but affects its proper localization in the tip, and finally deletion of *kipA* leads to spreading of TeaR along the tip membrane. These results suggest that TeaA mislocalization in the *kipA* mutant cannot be explained solely by the mislocalization or absence of TeaR but rather they suggest that KipA is transporting another protein, which is required for proper localization of TeaR. This is supported also by the different hyphal phenotypes of the mutants. Whereas *kipA* and *teaR* deletion produce meandering hyphae, *teaA* deletion caused zig-zag growth. The identification of proteins transported by KipA should help to further unravel this puzzle.

In *A. nidulans*, a formin, SepA, characteristic for the *S. cerevisiae* polarisome, was detected at the tip membrane and in the Spitzenkörper. This suggested, that the Spitzenkörper represents an organelle consisting of vesicles but also proteins, in addition to actin, required for the organization of the actin cytoskeleton (Sharpless and Harris, 2002; Harris *et al.*, 2005). Here, we identified that TeaA and TeaR localized to tips and accumulated at one point at the apex, which colocalized with the Spitzenkörper stained with FM4-64, whereas the accumulation at one point is not observed in Tea1 and Mod5 of *S. pombe*. However, the resolution of the localization of the proteins and the Spitzenkörper may not be sufficient to really determine whether the proteins are components of the Spitzenkörper. There is evidence that TeaA and TeaR are not closely associated with this organelle. We found that the TeaA point at the tip was resistant to cytochalasin A treatment, whereas the Spitzenkörper dissolved. In contrast, SepA localization was affected by cytochalasin A. In *C. albicans*, it was suggested that the Spitzenkörper and the polarisome protein complex are distinct structures in the tip of growing hyphae (Crampin *et al.*, 2005). Thus, it could be that TeaA and TeaR define a protein

complex in *A. nidulans* overlapping with but being distinct from the Spitzenkörper.

Our yeast two-hybrid and BiFC experiments demonstrated interaction between TeaA and TeaR. TeaA and TeaR often colocalized at the tips, but the localization was not always the same, and the TeaA point could temporarily localize to tips independently of TeaR. One explanation could be that only a fraction of TeaR interacts with TeaA. Furthermore, it has to be considered that TeaR localization was also dependent on TeaA, suggesting that TeaA could be anchored independently of TeaR at the membrane. Likewise, we found that filipin treatment first affects TeaR localization without changing obviously the localization of TeaA. Another possibility is that upon filipin treatment the interaction of TeaA and TeaR is disrupted, and TeaA just remains close to the membrane.

Although TeaA localization at tips depends on MTs, TeaA at the tips also plays a role in the regulation of MT dynamics. In the *teaA*-deletion mutant, some MTs did not converge at tips and other MTs failed to stop growing after reaching the tips and bent. Several proteins have been identified to regulate the MT plus-end dynamics referred to +TIPs in eukaryotic cells. In *S. pombe*, one of the +TIPs, CLIP-170 homologue Tip1 is revealed to interact with Tea1 at MT plus ends (Feierbach *et al.*, 2004). Interactions of TeaA with +TIPs in *A. nidulans*, such as ClipA and AlpA corresponding to CLIP-170 and Dis1/XMAP215 (Efimov *et al.*, 2006; Enke *et al.*, 2007), have to be analyzed. In the *kipA* mutant, the TeaA point at tips sometimes divided into a few points and MTs attached to the TeaA points (Figure 5E), suggesting TeaA accumulation at one point is associated with the convergence of MTs at the tips. The convergence of MTs at tips is possibly involved in the formation of the Spitzenkörper, because it is thought that MTs are necessary for long-distance vesicle transport toward the Spitzenkörper (Schuchardt *et al.*, 2005).

The effect of filipin on the distribution of the two cell-end markers, TeaA and TeaR, suggests an important role of sterol-rich microdomains in the membrane for localized insertion of the cell end factors (Alvarez *et al.*, 2007). Filipin has a specific affinity for sterols; thus, it integrates into regions with high sterol contents. Thereby, it possibly disturbs the structure of the membrane and, in our case, causes the mislocalization of TeaA and TeaR. There have been reports that sterol-rich lipid microdomains may play important roles in polarized growth in fungi, because they were detected in *C. neoformans* at bud tips and at protrusions that elongate to conjugation tubes during mating and at the tips of mating projections in *S. cerevisiae* and *S. pombe* (Bagnat and Simons, 2002; Nichols *et al.*, 2004; Wachtler and Balasubramanian, 2006). However, a link between the cell end markers and the membrane domains was missing. Recently, another tip-localized membrane protein was described in *A. nidulans*, MesA (Pearson *et al.*, 2004). This protein contains predicted transmembrane domains, and it is necessary for the stable recruitment of SepA. Whether the sterol-rich microdomains are also necessary for localization of this protein and whether it interacts with the TeaA–protein complex, remains to be uncovered.

ACKNOWLEDGMENTS

REFERENCES

Alvarez, F. J., Douglas, L. M., and Konopka, J. B. (2007). Sterol-rich plasma membrane domains in fungi. Eukaryot. Cell *6*, 755–763.

Bagnat, M., and Simons, K. (2002). Cell surface polarization during yeast mating. Proc. Natl. Acad. Sci. USA *99*, 14183–14188.

Browning, H., Hackney, D. D., and Nurse, P. (2003). Targeted movement of cell end factors in fission yeast. Nat. Cell Biol. *5*, 812–818.

Browning, H., Hayles, J., Mata, J., Aveline, L., Nurse, P., and McIntosh, J. R. (2000). Tea2p is a kinesin-like protein required to generate polarized growth in fission yeast. J. Cell Biol. *151*, 15–27.

Busch, K. E., Hayles, J., Nurse, P., and Brunner, D. (2004). Tea2p kinesin is involved in spatial microtubule organization by transporting tip1p on microtubules. Dev. Cell *16*, 831–843.

Chang, F., and Peter, M. (2003). Yeasts make their mark. Nat. Cell Biol. *5*, 294–299.

Crampin, H., Finley, K., Gerami-Nejad, M., Court, H., Gale, C., Berman, J., and Sudbery, P. (2005). *Candida albicans* hyphae have a Spitzenkörper that is distinct from the polarisome found in yeast and pseudohyphae. J. Cell Sci. *118*, 2935–2947.

Dietrich, F. S. *et al.* (2004). The *Ashbya gossypii* genome as a tool for mapping the ancient *Saccharomyces cerevisiae* genome. Science *304*, 304–307.

Efimov, V., Zhang, J., and Xiang, X. (2006). CLIP-170 homologue and NUDE play overlapping roles in NUDF localization in *Aspergillus nidulans*. Mol. Biol. Cell *17*, 2021–2034.

Enke, C., Zekert, N., Veith, D., Schaaf, C., Konzack, S., and Fischer, R. (2007). *Aspergillus nidulans* Dis1/XMAP215 protein AlpA localizes to spindle pole bodies and microtubule plus ends and contributes to growth directionality. Eukaryot. Cell *6*, 555–562.

Feierbach, G., Verde, F., and Chang, F. (2004). Regulation of a formin complex by the microtubule plus end protein tea1p. J. Cell Biol. *165*, 697–707.

Fischer-Parton, S., Parton, R. M., Hickey, P. C., Dijksterhuis, J., Atkinson, H. A., and Read, N. D. (2000). Confocal microscopy of FM4-64 as a tool for analysing endocytosis and vesicle trafficking in living fungal hyphae. J. Microsc. *198*, 246–259.

Girbardt, M. (1957). Der Spitzenkörper von *Polystictus versicolor*. Planta *50*, 47–59.

Grove, S. N., and Bracker, C. E. (1970). Protoplasmic organization of hyphal tips among fungi: vesicles and Spitzenkörper. J. Bacteriol. *104*, 989–1009.

Harris, S. D., and Momany, M. (2004). Polarity in filamentous fungi: moving beyond the yeast paradigm. Fungal Genet. Biol. *41*, 391–400.

Harris, S. D., Read, N. D., Roberson, R. W., Shaw, B., Seiler, S., Plamann, M., and Momany, M. (2005). Polarisome meets Spitzenkörper: microscopy, genetics, and genomics converge. Eukaryot. Cell *4*, 225–229.

Hill, T. W., and Käfer, E. (2001). Improved protocols for *Aspergillus* minimal medium: trace element and minimal medium salt stock solutions. Fungal Genet. Newsl. *48*, 20–21.

Howard, R. J. (1981). Ultrastructural analysis of hyphal tip cell growth in fungi: Spitzenkörper, cytoskeleton and endomembranes after freeze-substitution. J. Cell Sci. *48*, 89–103.

Kang, P. J., Sanson, A., Lee, B.-Y., and Park, H. O. (2001). A GDP/GTP exchange factor involved in linking a spatial landmark to cell polarity. Science *292*, 1376–1378.

Karos, M., and Fischer, R. (1999). Molecular characterization of HymA, an evolutionarily highly conserved and highly expressed protein of *Aspergillus nidulans*. Mol. Genet. Genomics *260*, 510–521.

Knechtle, P., Dietrich, F., and Philippsen, P. (2003). Maximal polar growth potential depends on the polarisome component AgSpa2 in the filamentous fungus *Ashbya gossypii*. Mol. Biol. Cell *14*, 4140–4154.

Konzack, S., Rischitor, P., Enke, C., and Fischer, R. (2005). The role of the kinesin motor KipA in microtubule organization and polarized growth of *Aspergillus nidulans*. Mol. Biol. Cell *16*, 497–506.

Martin, S. G., and Chang, F. (2003). Cell polarity: a new mod(e) of anchoring. Curr. Biol. *13*, R711–R730.

Martin, S. G., and Chang, F. (2006). Dynamics of the formin for3p in actin cable assembly. Curr. Biol. *16*, 1161–1170.

Martin, S. G., McDonald, W. H., Yates, J. R., and Chang, F. (2005). Tea4p links microtubule plus ends with the formin for3p in the establishment of cell polarity. Dev. Cell *8*, 479–491.

Martin, S. W., and Konopka, J. B. (2004). Lipid raft polarization contributes to hyphal growth in *Candida albicans*. Eukaryot. Cell *3*, 675–684.

Mata, J., and Nurse, P. (1997). Tea1 and the microtubular cytoskeleton are important for generating global spatial order within the fission yeast cell. Cell *89*, 939–949.

Montegi, F., Arai, R., and Mabuchi, I. (2001). Identification of two type V myosins in fission yeast, one of which functions in polarized cell growth and moves rapidly in the cell. Mol. Biol. Cell *12*, 1367–1380.

Nelson, W. J. (2003). Adaptation of core mechanisms to generate cell polarity. Nature *422*, 766–774.

Nichols, C. B., Fraser, J. A., and Heitman, J. (2004). PAK kinases Ste20 and Pak1 govern cell polarity at different stages of mating in *Cryptococcus neoformans*. Mol. Biol. Cell *15*, 4476–4489.

Pearson, C. L., Xu, K., Sharpless, K. E., and Harris, S. D. (2004). MesA, a novel fungal protein required for the stabilization of polarity axes in *Aspergillus nidulans*. Mol. Biol. Cell *15*, 3658–3672.

Peñalva, M. A. (2005). Tracing the endocytic pathway of *Aspergillus nidulans* with FM4-64. Fungal Genet. Biol. *42*, 963–975.

Philippsen, P., Kaufmann, A., and Schmitz, H.-P. (2005). Homologues of yeast polarity genes control the development of multinucleated hyphae in *Ashbya gossypii*. Curr. Opin. Microbiol. *8*, 370–377.

Philips, J., and Herskowitz, I. (1998). Identification of Kel1p, a kelch-domain-containing protein involved in cell fusion and morphology in *Saccharomyces cerevisiae*. J. Cell Biol. *143*, 375–389.

Pringle, J. R., Bi, E., Harkins, H. A., Zahner, J. E., DeVirglio, C., Chant, J., Corrado, K., and Fares, H. (1995). Establishment of cell polarity in yeast. Cold Spring Harb. Symp. Quant. Biol. 729–744.

Rajendra, L., and Simons, K. (2005). Lipid rafts and membrane dynamics. J. Cell Sci. *118*, 1099–1102.

Riquelme, M., Reynaga-Peña, C. G., Gierz, G., and Bartnicki-García, S. (1998). What determines growth direction in fungal hyphae? Fungal Genet. Biol. *24*, 101–109.

Rothberg, K. G., Ying, Y.-S., Kamen, B. A., and Anderson, R.G.W. (1990). Cholesterol controls the clustering of the glycophospholipid-anchored membrane receptor for 5-methoyltetrahydrofolate. J. Cell Biol. *111*, 2931–2938.

Sambrook, J., and Russel, D. W. (1999). Molecular Cloning: A Laboratory Manual, Cold Spring Harbor, NY: Cold Spring Harbor Laboratory Press.

Schuchardt, I., Assmann, D., Thines, E., Schuberth, C., and Steinberg, G. (2005). Myosin-V, Kinesin-1, and Kinesin-3 cooperate in hyphal growth of the fungus Ustilago maydis. Mol. Biol. Cell *16*, 5191–5201.

Sharpless, K. E., and Harris, S. D. (2002). Functional characterization and localization of the *Aspergillus nidulans* formin SEPA. Mol. Biol. Cell *13*, 469–479.

Sheu, Y. J., Santos, B., Fortin, N., Costigan, C., and Snyder, M. (1998). Spa2p interacts with cell polarity proteins and signaling components involved in yeast cell morphogenesis. Mol. Cell. Biol. *18*, 4053–4069.

Snaith, H. A., Samejima, I., and Sawin, K. E. (2005). Multistep and multimode cortical anchoring of tea1p at cell tips in fission yeast. EMBO J. *24*, 3690–3699.

Snaith, H. A., and Sawin, K. E. (2003). Fission yeast mod5p regulates polarized growth through anchoring of tea1p at cell tips. Nature *423*, 647–651.

Snell, V., and Nurse, P. (1994). Genetic analysis of cell morphogenesis in fission yeast–a role for casein kinase II in the establishment of polarized growth. EMBO J. *13*, 2066–2074.

Toews, M. W., Warmbold, J., Konzack, S., Rischitor, P. E., Veith, D., Vienken, K., Vinuesa, C., Wei, H., and Fischer, R. (2004). Establishment of mRFP1 as fluorescent marker in *Aspergillus nidulans* and construction of expression vectors for high-throughput protein tagging using recombination in *Escherichia coli* (GATEWAY). Curr. Genet. *45*, 383–389.

Vienken, K., and Fischer, R. (2006). The $Zn(II)_2Cys_6$ putative transcription factor NosA controls fruiting body formation in *Aspergillus nidulans*. Mol. Microbiol. *61*, 544–554.

Virag, A., and Harris, S. D. (2006). Functional characterization of Aspergillus nidulans homologues of *Saccharomyces cerevisiae* Spa2 and Bud6. Eukaryot. Cell *5*, 881–895.

Wachtler, V., and Balasubramanian, M. K. (2006). Yeast lipid rafts? An emerging view. Trends Cell Biol. *16*, 1–4.

Wachtler, V., Rajagopalan, S., and Balasubramanian, M. K. (2003). Sterol-rich plasma membrane domains in the fission yeast Schizosaccharomyces pombe. J. Cell Sci. *116*, 867–874.

Wendland, J. (2003). Analysis of the landmark protein Bud3 of *Asbya gossypii* reveals a novel role in septum construction. EMBO Rep. *4*, 200–204.

Wendland, J., and Walther, A. (2006). Septation and cytokinesis in fungi. In: The Mycota, Growth Differentiation and Sexuality, Vol. I, ed. U. Kües and R. Fischer, Heidelberg, Germany: Springer, 105–121.

Wright, G. D., Arlt, J., Poon, W. C., and Read, N. D. (2007). Optical tweezer micromanipulation of filamentous fungi. Fungal Genet. Biol. *44*, 1–13.

Yelton, M. M., Hamer, J. E., and Timberlake, W. E. (1984). Transformation of *Aspergillus nidulans* by using a *trpC* plasmid. Proc. Natl. Acad. Sci. USA *81*, 1470–1474.

Zahner, J. E., Harkins, H. A., and Pringle, J. R. (1996). Genetic analysis of the bipolar pattern of bud site selection in the yeast *Saccharomyces cerevisiae*. Mol. Cell Biol. *16*, 1857–1870.

Zhang, J., Li, S., Fischer, R., and Xiang, X. (2003). Accumualtion of cytoplasmic dynein and dynactin at microtubule plus ends in Aspergillus nidulans is kinesin dependent. Mol. Biol. Cell *14* 1479–1488.